Solving Turbine Governor Instability at Low-Load Conditions

Scott Manson
Schweitzer Engineering Laboratories, Inc.

Bill Kennedy
BHP Billiton Worsley Alumina Pty Ltd.

Matt Checksfield
Powerplan Engineers Pty Ltd.

This paper was presented at the 62nd Annual Petroleum and Chemical Industry Technical Conference and can be accessed at: http://dx.doi.org/10.1109/PCICON.2015.7435099.

For the complete history of this paper, refer to the next page.

Published in
Wide-Area Protection and Control Systems: A Collection of Technical Papers Representing Modern Solutions, 2017

Originally presented at the
62nd Annual Petroleum and Chemical Industry Technical Conference, October 2015

SOLVING TURBINE GOVERNOR INSTABILITY AT LOW-LOAD CONDITIONS

Scott Manson
Senior Member, IEEE
Schweitzer Engineering Laboratories, Inc.
2350 NE Hopkins Court
Pullman, WA 99163, USA

Bill Kennedy
BHP Billiton Worsley Alumina Pty Ltd.
PO Box 344
Collie, WA 6225, Australia

Matt Checksfield
Powerplan Engineers Pty Ltd.
Suite 1, 43 Kirwan Street
Floreat, WA 6014, Australia

Abstract—During routine commissioning of a steam turbine load-sharing system, serious low-load frequency instabilities were discovered. These instabilities were causing undamped oscillations in power and frequency to escalate until protective relays tripped a generator offline. Root-cause investigation led to a robust solution and some rather startling revelations about the implications of electronic governor controls and small (micro) grids.

There are basically two ways to form an electronic governor control loop with droop: speed control with a MW droop or MW control with a speed droop. The analysis in this paper shows one method to be superior under low-load conditions.

The results of this analysis have implications for the frequency stability of the power grid today. Microgrids, green energy, distributed generation, and isolated industrial plants can all be susceptible to this instability.

The authors estimate that approximately 60 percent of generation today is prone to destabilize the power system frequency under low-load conditions.

Index Terms—Frequency instability, governor instability, oscillations.

I. INTRODUCTION

This paper shares the methods used to find root cause and solve a governor-induced frequency instability problem. The methodology employed by the team required disciplined investigation, research, mathematical reduction, modeling, and testing. These methods apply in general for anyone working to solve a similar problem. This paper describes the following ten-step process:

1. Data capture.
2. Data reduction.
3. Key observations.
4. Asking and listening.
5. Hypothesis.
6. Mathematical analysis.
7. Unifying explanation.
8. Proposing a solution.
9. Modeling.
10. Testing.

II. BACKGROUND

The frequency instability event described in this paper occurred at the industrial refinery facility depicted in Fig. 1. The instability occurred when the 30 MW rated Steam Turbine Generator C (STG-C) and 15 MW of process load were electrically separated from the main processing plant. The 15 MW of electrical load consisted primarily of direct-on-line-connected (DOL-connected) motors and variable speed drives (VSDs). STG-C and the load were part of a power system grid section that was completely isolated from all other electrical grid sections. This type of grid section is referred to as a grid island throughout this paper.

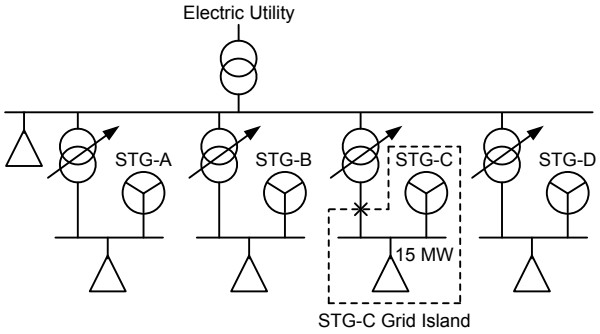

Fig. 1 Grid Islanding of STG-C

After the incident, power plant operators explained that such instabilities occurred sometimes, but not always, when STG-A, -B, or -C were grid-islanded in this manner. The instabilities had never been observed when STG-D was islanded. The problem had never been identified or corrected because it was inconsistent, it was unpredictable, and insufficient data were captured during prior events.

The intermittent instability problems started happening after the governors for STG-A, -B, and -C had been upgraded to modern digital governor controls. STG-A, -B, and -C had previously run for decades without problems with mechanical-type governors. STG-D had also been upgraded to a different type of digital governor control, and it was not exhibiting the frequency instability problems. Note that the STG-A, -B, and -C governors were from one manufacturer, and the STG-D governor was from another manufacturer.

The turbines from these two manufacturers were also of different construction. As depicted in Fig. 2, the turbines of STG-A, -B, and -C were of a three-stage-style extraction construction. STG-D was of a single-stage back-pressure construction. All four STGs were rated at approximately 30 MW.

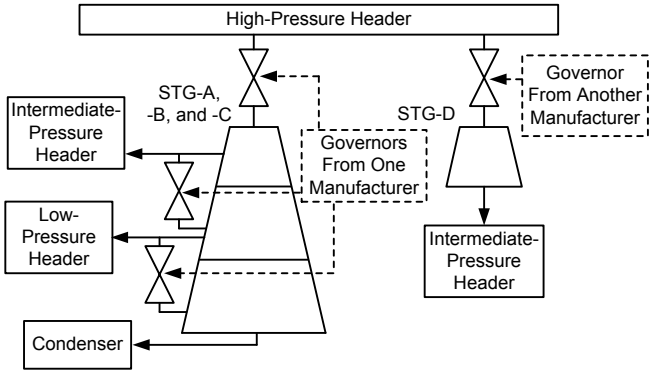

Fig. 2 Differing Turbine and Governor Technologies

The instability resulted in a loss of approximately 15 MW of plant processing equipment. The situation required an immediate investigation into why the event occurred.

III. DATA CAPTURE

STG-C was grid-islanded to commission and test the performance of a newly installed generator control system (GCS). The GCS automatically dispatches governor set points to maintain system frequency while simultaneously performing turbine load sharing. The GCS also includes exciter load sharing, optimal voltage control, and automatic synchronization systems. However, these systems are not relevant to this root-cause investigation, so further discussion is not included in this paper. For more information on GCS control strategies, refer to [1] and [2].

The GCS commissioning and testing required small-step testing of the governor set points to characterize the governor, turbine, and generator system. Previously, similar procedures were successfully run at many other facilities without incident.

During the islanding event, monitoring and plotting functions were enabled on the GCS controllers and governor controllers. Event report (oscillography) functionality was also enabled on protective relays throughout the plant. This recording was enabled in anticipation of performing the aforementioned GCS testing.

Frequency, power, and voltage data from protective relays throughout the plant were sent at 4-millisecond intervals to the GCS controller. The relays sent the data across an Ethernet local-area network (LAN) via the IEC 61850 Generic Object-Oriented Substation Event (GOOSE) protocol. These data were then downsampled to 50 milliseconds in the GCS controllers. The GCS controllers did not capture the time stamps of the IEC 61850 GOOSE messages because the time stamps were not relevant to the GCS control strategy.

Triggered oscillographic data from the relays were limited in time duration to a few power system cycles and therefore were not sufficient in duration for this analysis. This is because the oscillographic data in modern digital protective relays are optimized for capturing events associated with power system faults. The protective relays, therefore, captured voltage and current waveforms at sample rates of several kilohertz. The frequency oscillations observed in this instability phenomenon had a periodicity (time period) of 4.5 seconds (0.22 Hz), and several seconds of data capture, at a minimum, were required.

During the initial event, there were intermittent problems with data plotting in the governor software. These problems rendered some of the governor data questionable. The relay data sent to the GCS controllers were from in-service protective relays and thus were deemed sufficiently accurate and time-synchronized to become the basis of the initial observational data set.

After correcting the governor plotting problems, final data collection during the offline and online testing was performed with the governor. Plotting data from the governor was advantageous because it captured valve position signals from linear variable differential transformers, shaft speed measurements from a toothed wheel, and intermediate mathematical and logical data points internal to the governor.

Sequence of events (SOE) data from the relays located throughout the plant captured periodic underfrequency element pickups, overfrequency element pickups, and the eventual trip of the loads and generators. The SOE data were time-stamped to ±1-millisecond accuracy with Inter-Range Instrumentation Group time code format B (IRIG-B) satellite time synchronization.

Putting together the entire picture of what happened required manual time alignment of non-time-stamped data from the GCS controllers and time-stamped SOE data from the relays.

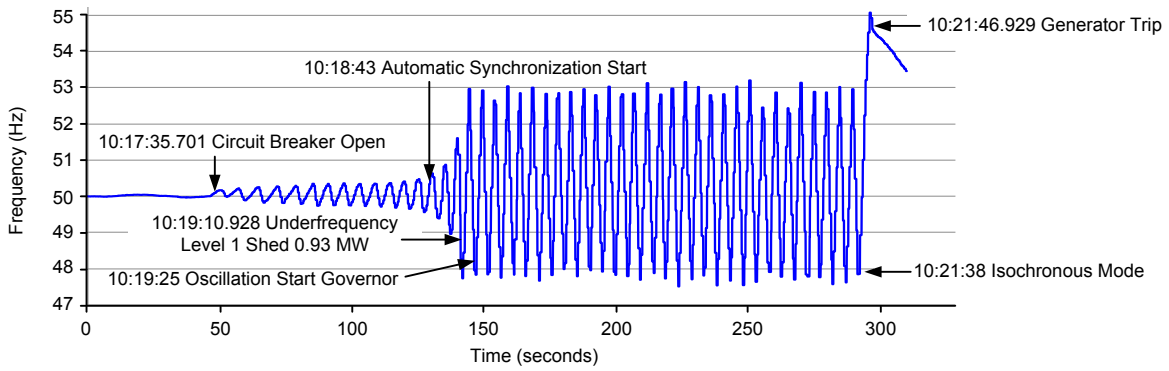

Fig. 3 Frequency Instability Plotted Versus Time (50-millisecond sample rate)

Fig. 3 is a plot from the GCS controller during the STG-C islanding event. Because the GCS controller data shown in Fig. 3 were not IRIG-B time-stamped, the absolute time stamps shown in Fig. 3 were derived by correlating SOE data from the relays with GCS analog data. This postmortem data analysis of the initial event took many hours and could have been avoided had all the digital and analog data been IRIG-B time-synchronized and centrally consolidated. The primary reason the stability problem had not been addressed earlier was because insufficient data had been captured during previous instability events. The technology used in electric transmission systems to capture data for inter-area oscillations would have been a perfect fit for capturing the data from this event [3].

In Fig. 4, the same event is plotted as frequency versus power. The initial oscillations can be seen as a circle around the 15 MW, 50 Hz location. The oscillations grew to the larger square-like shape as the valves ran from fully opened to fully closed. The center point of this square moved to less than 15 MW as load shedding reduced the total grid-island load.

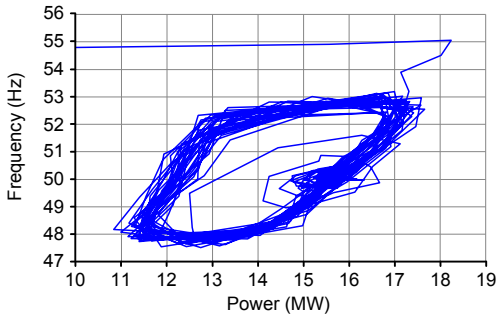

Fig. 4 Frequency Plotted Versus Power

IV. DATA REDUCTION

The second step in the root-cause analysis is to reduce several hundred megabytes of data into useful information. This activity required plotting trends, the time synchronization of data, long discussions with multidisciplinary teams, and reducing the data into a minimal set of information. The data were used to prove or reject a great number of hypotheses and speculations.

Table I summarizes the timeline of the plot from the GCS controller during the STG-C islanding event shown in Fig. 3.

TABLE I
EVENT TIMELINE

Time*	Event
10:17:35.701	The grid island started as the circuit breaker opened. Frequency oscillations of a 4.5-second period grew to ±0.3 Hz in amplitude.
10:18:43	Automatic synchronization systems started sending raise and lower signals to attempt to synchronize the breaker. Operators observed these oscillations and started sending raise and lower signals as well. The oscillations stayed at a 4.5-second period and started to grow.
10:19:10.928	Underfrequency load shedding tripped loads by correctly operating at 48.5 Hz. The oscillations stayed at a 4.5-second period and grew to ±2.5 Hz amplitude. The main high-pressure valves were visually observed to be oscillating from wide open to fully closed after this point.
10:21:38	Power plant operators switched the STG-C governor into isochronous mode. The frequency swung to 55 Hz.
10:21:46.929	Generator protection tripped the STG-C breaker, and the grid-island voltage collapsed.

* Note that events without millisecond-level time stamps did not have SOE data points.

V. KEY OBSERVATIONS

This root-cause analysis step includes listing a set of minimal and unique observations that summarize the event. There was insufficient evidence to determine root cause at this point; however, the list of key observations was essential for directing the future investigation into the correct root cause. Key observations document any contradictions, anomalies, or trends that are unexplained or concerning. These key observations required hours of discussions with plant engineers, technicians, operators, maintenance staff, and management.

The following key observations eventually led to an accurate root-cause analysis:

1. The lower the power output of the STG, the higher the likelihood that the oscillation would occur.

2. Oscillations did not occur when the system was grid-connected; they only occurred when the system was grid-islanded.
3. Not all grid-island formations caused instability.
4. Not all grid islands had the same composition of VSD- and DOL-connected motors. The relative percentage of VSD to DOL is referred to as the load composition throughout this paper.
5. The governors had no way of identifying that they were part of an islanded grid, yet somehow the STG-A, -B, and -C governors did not respond to set-point dispatch signals while grid-islanded and in droop mode.
6. The authors differed in regard to their experiences with droop controls. One author had never experienced frequency instability with turbines in grid islands. Another author had previously experienced several frequency instabilities with turbines in grid islands.
7. STG-D did not have similar stability or set-point issues like those experienced on STG-A, -B, and -C. The STG-D governor always operated in droop mode.
8. There had been intermittent and unexplained issues synchronizing with the local utility since the installation of the digital governors on STG-A, -B, and -C.
9. Most grid-island formations in the plant included multiple, parallel-connected STGs. Switching one STG to isochronous mode would not definitively solve the instability because one or more STGs would be forced to operate in droop on any island. Thus, a stable droop solution was required.
10. There was a 1-second single-pole low-pass filter (SPLPF) placed into the STG-A, -B, and -C governors on the speed feedback signal. This filter was inserted to alleviate some concerns about high-frequency noise. The SPLPF was not in service during prior STG islanding instability events.

VI. ASKING AND LISTENING

The asking and listening step is the point in the process that most often stops a team from determining root cause. It requires the consulting engineer to have detailed conversations with dozens of personnel from all parts of an organization. These conversations are best documented with sketches and notes. The creativity, experience, and patience involved with this step are significant.

This step was accomplished simultaneously with a thorough review of all governor, exciter, turbine, generator, steam system, electrical load, and associated documentation. Code reviews of the governor, exciters, and process control systems were required. Physical inspections of the turbines, hydraulic equipment, and steam valves were required.

This step is where it is important to determine what the documentation does not show. It is uncommon to find an organization with documentation that is 100 percent complete, up to date, or easy to locate. Electricians who corrected problems, engineers who observed prior instabilities, operations personnel on shift during the last instability, process control engineers, and shift supervisors with decades of power plant experience were key to the discussions in this case.

The output of this step in the process was an accurate summary of the entire STG-A, -B, and -C system in question in a single drawing. This drawing was further simplified for Fig. 5. Another similar diagram was created for STG-D but is not included here. It takes experience with similar problems to determine how much detail on the hydraulics must be documented, which pieces of the process control algorithms are pertinent, and how to summarize complex governor code.

Standard IEEE, ISA, ASME, and IEC symbology was not used in Fig. 5 due to the extreme simplification that had to occur and also because the diagram had to be easily understood by a large number of plant employees with differing skill levels.

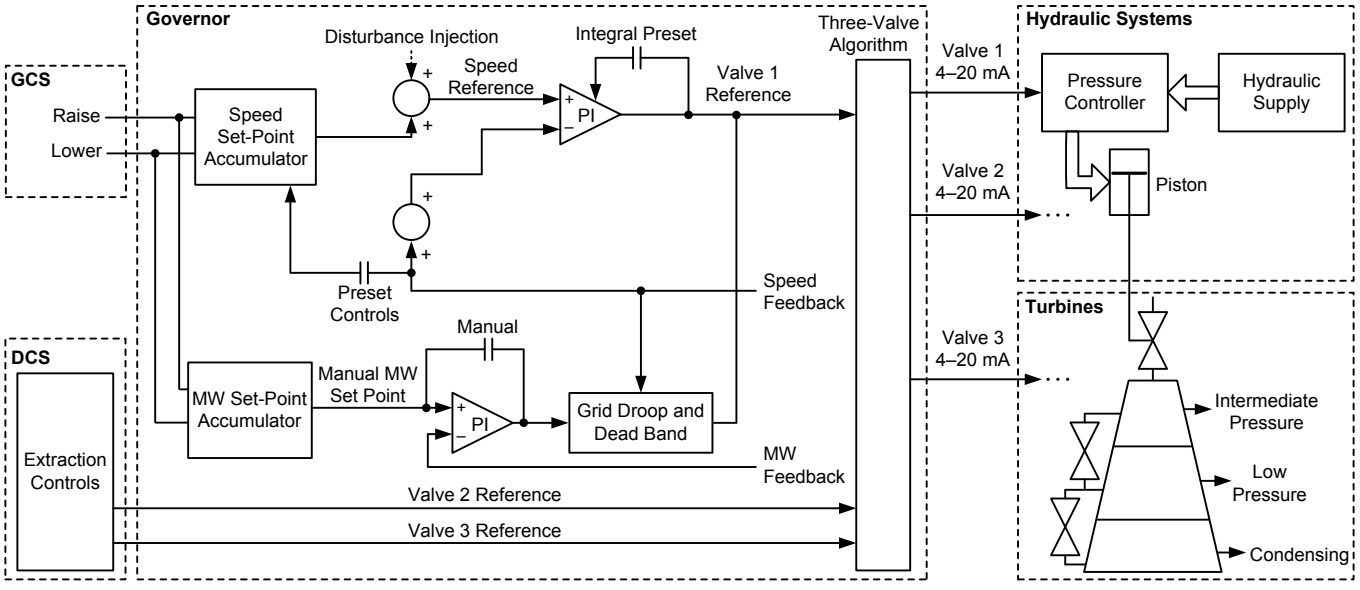

Fig. 5 Simplified Turbine, Governor, Hydraulic, Distributed Control System (DCS), and GCS Interface

VII. HYPOTHESIS

The authors suspected that the STG-A, -B, and -C governor algorithms were at the root of the problem.

The STG-A, -B, and -C governors had a proportional integral derivative-based (PID-based) power (MW) control system with a speed (revolutions per minute [rpm]) droop term, as shown in Fig. 6. One of the authors had experienced low-load islanded frequency instability problems with other STGs governed in this manner.

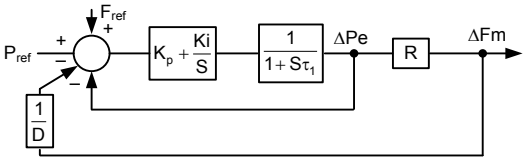

Fig. 6 STG-A, -B, and -C Block Diagram

The STG-D governor had a PID-based speed (rpm) control system with a power (MW) droop term, as shown in Fig. 7. The authors had never experienced low-load islanded frequency instability problems with this form of governor control at generation plants.

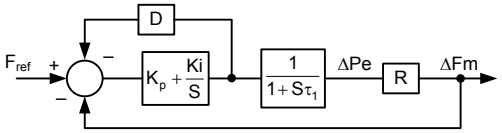

Fig. 7 STG-D Block Diagram

VIII. MATHEMATICAL ANALYSIS

In this step, a mathematical comparison between the STG-A, -B, and -C and the STG-D governor algorithms was performed. This was accomplished by reducing Fig. 5 into simple block diagrams (Fig. 6 and Fig. 7).

Fig. 6 and Fig. 7 were confirmed to be accurate (validated) through rigorous analysis. After this validation step, a large number of mathematical analyses were performed to compare the block diagrams. One of the many analyses performed appeared to provide a unifying explanation for all the observed phenomena.

The analysis that led to the root cause was a sensitivity analysis of the net system transfer function gain as a ratio of actual versus set-point frequency.

To accomplish the sensitivity analysis, Fig. 6 and Fig. 7 were reduced to the transfer functions shown in (1) and (2), respectively. The net gain of the system is evaluated by assuming the signals are dc. This allows the single time constant elements to be replaced with a one. Integral gains are set to zero for this form of analysis. Equation (1) is the STG-A, -B, and -C transfer function. Equation (2) is the STG-D transfer function.

$$\left.\frac{\Delta Fm}{F_{ref}}\right|_{\substack{Ki=0\\dc}} = \frac{RD}{D+R} \tag{1}$$

$$\left.\frac{\Delta Fm}{F_{ref}}\right|_{\substack{Ki=0\\dc}} = \left(\frac{R}{\frac{1}{K_p}+D+R}\right) \tag{2}$$

Equations (1) and (2) show the response of the actual power system frequency to a small (incremental) change in the frequency set point. Sensitivity analysis is applied to the transfer functions of (1) and (2) by varying the parameters *R*, *D*, and K_p. These are defined as follows:

1. 1/R is the incremental change in load real power consumption that will occur if the present electrical power system frequency increases slightly. Units for *R* are Hz/MW.
2. *D* is the droop setting in the governors. This was 5 percent for both governors. Units for *D* are per unit (pu) frequency/pu power.
3. K_p is the proportional gain of the PID speed control loop in the STG-D governor. Units for K_p are MW/Hz.

Note that several of the parameters shown in Fig. 6 and Fig. 7 are not described or listed here because they are not pertinent to the final transfer functions, as shown in (1) and (2). These extra parameters are shown in Fig. 6 and Fig. 7 to help the reader understand the simplification process.

The *R* (Hz/MW) of the power system loads is critical in this analysis. During prior power system stability studies, 1/R was found to vary from 1.5 to 14 MW/Hz for the islanded plant. The study did not examine the 1/R of the grid-connected plant. Data points on 1/R were collected at three points: 14 MW, 200 MW, and utility grid connected. The data points from the field observations and the study are plotted together in Fig. 8.

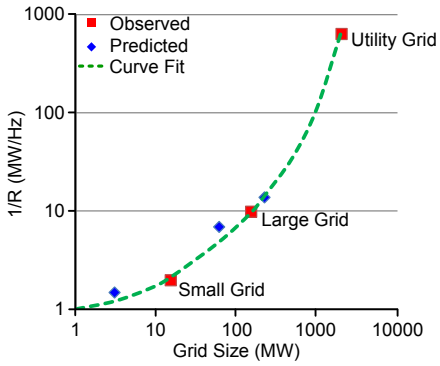

Fig. 8 1/R Plotted Versus Islanded Grid Load

As discovered during the studies and field observations, 1/R values vary as a function of the size of the islanded electrical load and as a function of the load composition. Smaller electrical loads and greater percentages of VSD on the islanded grid reduce 1/R (i.e., they make the system more sensitive to changes in STG mechanical power input). Should the entire plant separate from the local utility as a single power system island, 14 MW/Hz was proven to be an accurate estimate. Should a single STG separate from the local utility with approximately 3 MW of electrical load, 1.5 MW/Hz was proven to be an accurate estimate.

The 1/R values determined during power system stability studies were validated during observations of prior STG-C grid-island events that did not result in instability. There was no instability detected in these prior tests because the governor was in extraction mode instead of droop mode. During those tests, a 1 MW output increase from STG-C was found to change the islanded grid frequency by about 0.5 Hz during an island condition of about 23 MW. This equates to a 2.0 MW/Hz value, as shown in Fig. 8.

Sensitivity analysis was performed by evaluating the net system gain of the transfer functions of (1) and (2) as a function of grid size (MW). In Fig. 9, the upper line is the net gain of (1) (STG-A, -B, and -C) and the lower line is the net gain of (2) (STG-D). These curves were derived with the valid assumption that the K_p gain is much lower than 1/D.

Note that during the mathematical reductions of the STG-A, -B, and -C governors, it was discovered that there was a defect in the dead-band algorithm used for droop control. This defect fully accounted for why STG-A, -B, and -C did not respond to set-point changes under islanded mode conditions that the governors could not detect. It also explained why the STG would not always synchronize properly in droop mode. This defect had no influence, however, on the frequency instability described herein; they were two separate defects.

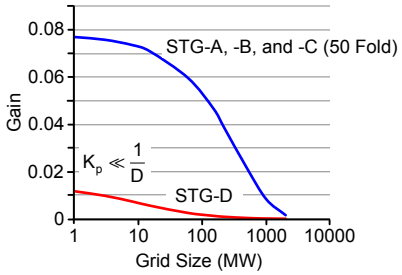

Fig. 9 Net System Gain as a Function of Grid Size

IX. UNIFYING EXPLANATION

Closed-loop control systems that are tuned to be stable under one set of conditions can become unstable under conditions that increase the net system gain.

The authors knew from prior experience that excessive net system gain will cause speed instabilities in a governor. The combined effect of high controller gains and nonlinear systems is commonly oscillation and/or instability. High net system gains should always be avoided if possible because they also wear out mechanical equipment. System lags, hysteresis, hard limits, valve stiction, and rate limits, which are part of any mechanical or hydraulic system, will compound instabilities under high gain conditions.

Fig. 9 shows that the STG-A, -B, and -C governors exhibit approximately a 50-fold increase in net system gain at low-load island conditions, as compared with utility-connected grid conditions. The STG-D governor will only exhibit this increase in net system gain if K_p approaches 1/D. STG-D is therefore insensitive to low-load conditions, while STG-A, -B, and -C are very sensitive.

This analysis indicated that a governor speed loop with a MW droop term can be tuned with a single set of gains to be stable for all sizes of grid islands and load compositions. It also indicated that this is not possible for a MW loop with a speed droop term.

Further corroborating this explanation was the fact that the 1-second SPLPF on the speed feedback appeared to worsen the magnitude of the frequency and power oscillations. Prior to the STG-C islanding event in question, STG-A, -B, and -C were shown to be unstable at below approximately 7 MW without an SPLPF. With the SPLPF, the governor was found to be unstable at 15 MW. It was speculated that an easy way to find the tendencies of a governor for low-load island instability would be to insert artificial low-pass filters on rpm speed feedback during governor commissioning.

X. PROPOSING A SOLUTION

The proposed solution to solve the instability included rewriting portions of the STG-A, -B, and -C governor control code. Several alternative solutions were considered. After great deliberation, the alternate droop mode of control shown in Fig. 10 was selected. There were several pros and cons to be considered for this solution.

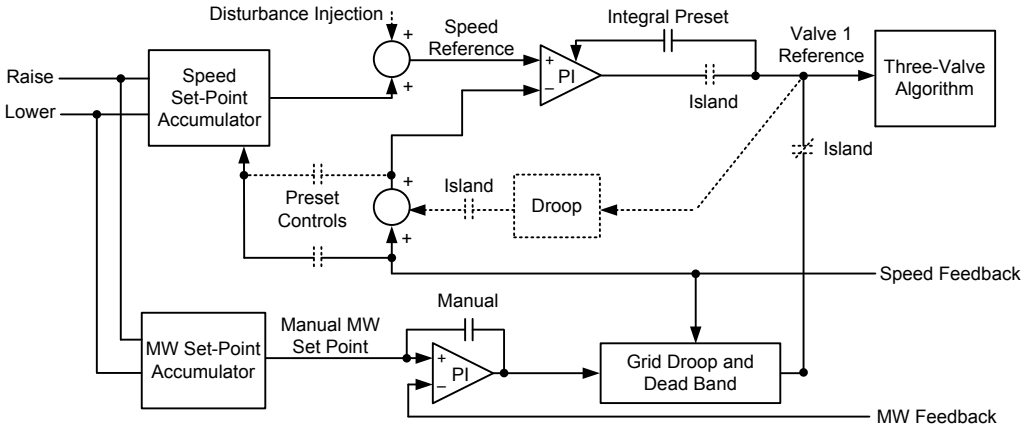

Fig. 10 Alternate Droop Solution

The STG-A, -B, and -C governors included an isochronous speed loop that was used during STG startup. This observation led to the consideration of forming an alternate droop governor control system by adding a MW droop term to the isochronous speed loop. The alternate droop method had the distinct advantage of being immune to low-load island conditions because the isochronous speed loop was known to be stable under no-load conditions.

The proposed alternate droop solution would bypass governor extraction mode control during island conditions. However, this was acceptable and preferable because of known dangers with operating an STG in extraction mode during grid-island conditions [2].

The proposed alternate droop solution is required to be switched into service whenever the GCS detects an island condition. The GCS is well suited for island detection because it is receiving the statuses of all the plant breakers and isolators from protective relays throughout the plant.

The droop line for the newly proposed alternate droop solution could be derived from either a live real power measurement or the valve reference. The valve reference method was chosen after great deliberation. The changes to the governor are summarized by the dotted lines in Fig. 10.

Using a valve reference droop line calculation will result in the total system droop exceeding the *D* value programmed in the governor. *R* will dominate the perceived droop on an islanded electrical grid when grid R > D. This is summarized for the power system in question in Table II. A larger-than-programmed droop behavior was not considered a major concern because the GCS dispatched the governor set point for frequency control.

TABLE II
SYSTEM DROOP FOR A VALVE SET-POINT DROOP LINE

	Grid-Connected Scenario	**Grid-Islanded Scenario**
Load (MW)	2,000	7
τ_2 (seconds)	0.6	1.0
R (rpm/MW)	0.33	30
D (rpm/MW)	5	5
Perceived Droop (rpm/MW)	5	30

Using a valve reference droop line calculation results in sensitivity to valve nonlinearity. These nonlinearities were determined to reduce the governor droop from 5 to 3 percent as the valves became fully open. The hydraulic controllers shown in Fig. 5 contained valve compensation that was only partially able to map out the valve position versus flow rate nonlinearity. A 2 percent reduction in droop was not considered a significant problem.

The overriding factor in selecting the valve reference droop line calculation technique was that it would not add further oscillations to an already unstable system. Using a measured power value for the droop line can introduce additional oscillatory modes into a governor speed control system. These situations occur because of high net system gain conditions and large lags in the power measurement and valve control hydraulics.

XI. MODELING

Adding the alternate droop control to STG-A, -B, and -C required significant fundamental changes to the governor logic and therefore required lengthy offline testing prior to testing on a live power system.

The STG-A, -B, and -C governors had the ability to run in an offline simulation environment. Using this offline simulation environment required the creation of a simplified model of an electric power system that adequately characterized load, generator, and turbine inertias as well as varying power system *R* values. This model is shown in Fig. 11.

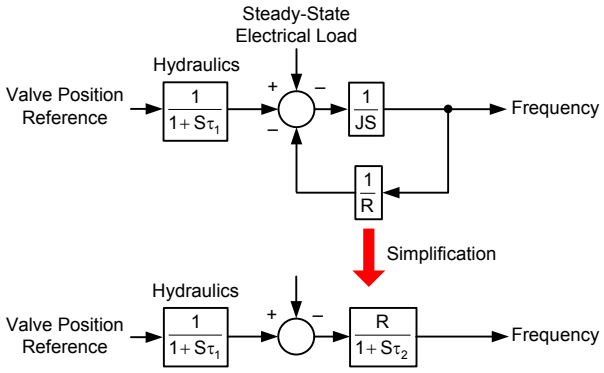

Fig. 11 Simplified Power System Model

In Fig. 11, τ_1 and τ_2 are the valve hydraulic time constant and the grid frequency time constant, respectively. τ_1 is approximately 1 second. τ_2 is equal to the inertia (J) multiplied by the *R* of a power system.

The model of Fig. 11 indicated that for the STG-A, -B, and -C governors, a net gain increase of 50 fold was also accompanied by an 8-fold increase of the power system time constant. Control engineers worldwide can relate to what these increases in gain and process time constant will do to a closed-loop control system. These increases in gain and time constant erode phase and gain margins, making control systems unstable.

To accurately model the STG governor connected to local utility power and in islanded operation, further measurements were taken from live test data, as summarized by the τ_2 and *R* values in Table II.

For modeling purposes, the local utility power system was assumed to have an *R* of approximately 0.33 rpm/MW and a subsequent grid frequency time constant (τ_2) of approximately 0.6 seconds. The plant was assumed to have an *R* of 30 rpm/MW and τ_2 of 1.0 second during a 7 MW load condition with average load composition. These units were translated from hertz to rpm for ease of modeling.

XII. TESTING

To validate the STG-A, -B, and -C governor code changes, the following tests were run offline in simulation mode:

1. Confirm that the newly devised alternate droop control method is stable under all load compositions and inertias.
2. Confirm that the alternate droop control method follows a 5 percent droop.
3. Verify that the governor moves between operational modes with bumpless transfer for all possible mode changes.
4. Confirm that the alternate droop control method follows set points and properly synchronizes.
5. Confirm that all other modes of operation are not affected by the new alternate droop control.
6. Inject disturbances into the governor, and confirm that the system is critically damped in the alternate droop control mode under worst-case load composition and inertial situations.
7. Simulate starting and stopping the largest loads to confirm that the system is critically damped in the alternate droop control mode.
8. Create and test a tuning procedure to be used during online testing.
9. Recreate the exact circumstances of the initial instability, and turn the frequency instability off.
10. Turn the instability on and off by switching the governor between the original control system and the new alternate droop control scheme.

All of the aforementioned tests were performed and documented to the satisfaction of facility personnel. The new alternate droop controls were found to match the predicted theory included in (1) and (2).

Fig. 12 shows the results of Test 9. Note that the frequency instability started as in Fig. 3, but this time, the new alternate droop control was switched in and the power system regained stability.

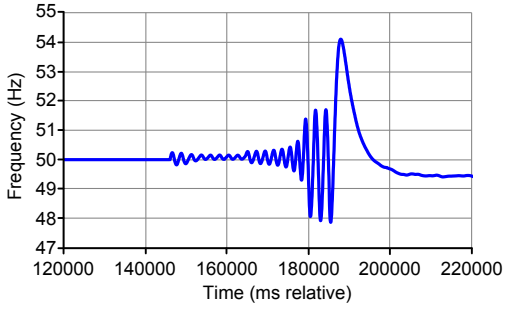

Fig. 12 Turning Frequency Instability Off

Fig. 12 also shows the governor operating in a stable state until islanded mode conditions were initiated. The initiation of the islanded model immediately caused the generator speed to start oscillating. Raise pulses were then applied at 30 and 60 seconds; these caused the ringing to worsen. A large block of load was removed to simulate the underfrequency load-shedding event, and the oscillations grew to ±100 rpm. The governor was then switched to alternate droop mode, and the oscillations settled down. Several minutes later, the GCS brought the frequency (speed) to nominal.

XIII. CONCLUSIONS

The alternate droop governor control system performed on the live system as the mathematical analysis and offline testing predicted. No frequency instabilities have occurred since the system was put into continuous operation in July 2013.

The following conclusions were made based on the information discussed in this paper:

1. The ten-step procedure described in this paper can be used to find the root cause of frequency instability problems on any size of electric power system.
2. The frequency instability in this case was caused by a low-load grid island. The grid-island load composition and inertia caused the net closed-loop gain to increase approximately 50 fold and the closed loop system time constant to increase by approximately 8 fold.
3. The STG governor logic contained an original equipment manufacturer defect that prevented the STGs from responding to set-point dispatch commands when islanded and in droop mode. This defect explained why the STGs would not always synchronize properly. This problem is avoided by using the new alternate droop governor control system.
4. A governor with a speed loop control and MW droop that works perfectly in island conditions can be sluggish but acceptable when grid-connected.
5. A governor with a MW loop control and speed droop can be fast and responsive in grid-connected mode but can also be unstable when islanded.
6. Detecting grid islanding and load composition is required to prevent low-load instabilities for most STGs.
7. The alternate droop control uses valve reference instead of active power measurements to ensure stability.
8. Electronic loads such as VSDs can destabilize turbine governor speed control systems. This is because they have a zero value of 1/R (their power consumption is constant) and zero inertia as reflected into the power system.

9. These frequency instability conditions are not isolated to industrial facilities. They are predicted to occur for utility microgrids as well.
10. Periodic performance-based testing of governors and turbines followed by data evaluation can detect and prevent these frequency instabilities in power systems.
11. The capture of time-synchronized and centrally consolidated analog and digital data throughout the governors, exciters, and relays would have assisted plant engineers in finding and correcting these problems earlier.
12. In the authors' experience, most steam and combined-cycle turbines have MW loop control while most hydro and gas turbines have speed loop control. From this, it can be estimated that approximately 60 percent of generation today is prone to low-load instability problems.

XIV. REFERENCES

[1] A. Upreti, S. M. Manson, and M. J. Thompson, "Case Study: Smart Automatic Synchronization in Islanded Power Systems," proceedings of the Power and Energy Automation Conference, Spokane, WA, March 2013.

[2] S. Manson, M. Checksfield, P. Duffield, and A. Khatib, "Case Study: Simultaneous Optimization of Electrical Grid Stability and Steam Production," proceedings of the 61st Annual Petroleum and Chemical Industry Technical Conference, San Francisco, CA, September 2014.

[3] E. O. Schweitzer, III, D. Whitehead, A. Guzmán, Y. Gong, and M. Donolo, "Advanced Real-Time Synchrophasor Applications," proceedings of the 35th Annual Western Protective Relay Conference, Spokane, WA, October 2008.

XV. VITAE

Scott Manson, P.E. (S 1991, M 1993, SM 2012), received his M.S.E.E. from the University of Wisconsin–Madison and his B.S.E.E. from Washington State University. Scott is presently the engineering services technology director at Schweitzer Engineering Laboratories, Inc.. In this role, he provides consulting services on control and protection systems worldwide. He has experience in power system protection and modeling, power management systems, remedial action schemes, turbine control, and multiaxis motion control for web-lines, robotic assembly, and precision machine tools. Scott is a registered professional engineer in Washington, Alaska, North Dakota, Idaho, and Louisiana. He can be contacted at scott_manson@selinc.com.

Bill Kennedy received his City and Guilds (London) Process Control Technicians certificate from the Rotherham College of Technology in Yorkshire, England. After 7 years with British Steel in Rotherham, England, Bill migrated to Australia in 1978 and joined Alcoa, spending 18 years in various roles in instrumentation and control engineering. After leaving Alcoa in 1996, Bill spent the next 2 years as a support manager for Vector International and Motherwell Systems in Perth. In 1998, Bill became an independent consultant and has worked on various projects, specializing in boiler and turbine control. He can be contacted at william.kennedy@bhpbilliton.com.

Matt Checksfield received his B.Eng. and Ph.D. in electronic and electrical engineering from the University of Bath in the UK. Matt worked for a UK generation consultancy, Power Technology, before migrating to Perth, Australia, in 2003 to work for Powerplan Engineers Pty Ltd. Matt has experience in the development of protective relays, plant condition monitoring and testing, protection system design, power system load flow, fault level and dynamic stability modeling, and power plant maintenance strategy. He has worked at generation and distribution utilities, renewable generation facilities, and industrial mine sites. Matt is a member of the Institution of Engineers Australia and is a chartered professional engineer in Australia. He can be contacted at matt.checksfield@powerplan.com.au.

Previously presented at the 62nd Annual Petroleum and Chemical Industry Technical Conference, Houston, TX, October 2015.

20150410 • TP6634